Available online at www.sciencedirect.com
SCIENCE DIRECT®
Journal of Organometallic Chemistry 690 (2005) 1763–1771
Journal of Organometallic Chemistry
www.elsevier.com/locate/jorganchem

Synthesis of $[Ni(\eta^2\text{-}CH_2C_6H_4R\text{-}4)\{PPh(CH_2CH_2PPh_2)_2\}]^+$ (R = H, Me or MeO) and protonation reactions with HCl

Valerie Autissier, Ellie Brockman, William Clegg, Ross W. Harrington, Richard A. Henderson *

Department of Chemistry, School of Natural Sciences, University of Newcastle, Newcastle upon Tyne NE1 7RU, UK

Received 7 December 2004; accepted 14 January 2005
Available online 8 March 2005

Abstract

The complexes $[Ni(\eta^2\text{-}CH_2C_6H_4R\text{-}4)(triphos)]BPh_4$ {R = H, Me or MeO; triphos = $PhP(CH_2CH_2PPh_2)_2$} have been prepared and characterised by spectroscopy and X-ray crystallography. In all cases the coordination geometry of the nickel is best described as square-planar with an η^2-benzyl ligand occupying one of the positions. The orientation of the η^2-benzyl ligand is dictated by the steric restrictions imposed by the phenyl groups on the triphos ligand, so that the phenyl group on the unique secondary phosphorus and the aromatic group of the benzyl ligand (which are *trans* to one another) are oriented in the same direction. $[Ni(\eta^2\text{-}CH_2C_6H_4R\text{-}4)(triphos)]^+$ react with an excess of anhydrous HCl in MeCN to form $[NiCl(triphos)]^+$ (characterised as the $[BPh_4]^-$ salt by X-ray crystallography) and the corresponding substituted toluene. The kinetics of the reaction of all $[Ni(\eta^2\text{-}CH_2C_6H_4R\text{-}4)(triphos)]^+$ and HCl in the presence of Cl^- have been determined using stopped-flow spectrophotometry. All reactions exhibit a first-order dependence on the concentration of complex and a first-order dependence on the ratio $[HCl]/[Cl^-]$. Varying the 4-R-substituent on the benzyl ligand shows that electron-withdrawing substituents facilitate the rate of the reaction. It is proposed that the mechanism involves initial rapid protonation at the nickel to form $[NiH(\eta^2\text{-}CH_2C_6H_4R\text{-}4)(triphos)]^{2+}$, followed by intramolecular proton migration from nickel to carbon to yield the products.

Keywords: Nickel; Benzyl; Protonation; Mechanism

1. Introduction

Studies on the kinetics of protonation of transition metal complexes are of fundamental interest in understanding the mechanisms of proton transfer to inorganic complexes as well as being relevant to the action of certain industrially important catalysis, such as hydrocyanation [1]. Whilst there have been significant advances in understanding the mechanisms of protonation of transition metal complexes, the following aspects are still unresolved [2]. (i) The electronic and steric factors which control the rate of protonation of metal complexes. Understanding these factors will allow us to predict the sites of protonation in new reactions. (ii) Elucidation of the kinetically favoured site of protonation of the complex, in particular, investigating whether a proton binds directly to the site identified in the product, or whether the proton binds initially to some other site (kinetically controlled product) and then moves to the ultimate site (thermodynamically controlled product). (iii) Probing the pathways by which protons move between the kinetically favoured and the thermodynamically favoured sites. These pathways can be intramolecular or intermolecular.

Earlier work from our laboratories focussed on the protonation of complexes based on the substitutionally robust $\{M(Ph_2PCH_2CH_2PPh_2)_2\}$ (M = Mo or W) core,

* Corresponding author. Tel.: +44 191 222 6636; fax: +44 191 222 6929.
E-mail address: r.a.henderson@ncl.ac.nk (R.A. Henderson).

0022-328X/$ - see front matter © 2005 Elsevier B.V. All rights reserved.
doi:10.1016/j.jorganchem.2005.01.034

containing a variety of different ligands such as N_2, RCN, RNC, alkyne or alkene [2,3]. More recently we have been studying the protonation reactions of complexes based on the $\{Ni(triphos)\}^+$ {triphos = PhP$(CH_2CH_2PPh_2)_2$} site, containing methyl [4], η^3-allyl [5] or thiolate [6] ligands. In particular, a study of the kinetics of the the reaction between $[NiMe(triphos)]^+$ and HCl to form methane {Eq. (1)}, indicates that although initial protonation occurs at the nickel, formation of methane has to await the subsequent direct protonation of the methyl ligand [4]. Intramolecular migration of hydrogen from nickel to methyl appears to be slow.

$$[NiMe(triphos)]^+ + HCl \rightarrow [NiCl(triphos)]^+ + CH_4 \quad (1)$$

In order to more fully understand the factors affecting the protonation of nickel alkyl complexes we have prepared and structurally characterized $[Ni(\eta^2\text{-}CH_2C_6H_4R\text{-}4)(triphos)]^+$ (R = H, Me or MeO) and studied the kinetics of the reactions of these complexes with HCl in MeCN.

2. Experimental

All preparations and manipulations were routinely performed under an atmosphere of dinitrogen using Schlenk or syringe techniques as appropriate. All solvents were dried and distilled under dinitrogen immediately prior to their use. Tetrahydrofuran (THF) was distilled from Na/benzophenone, diethyl ether (Et_2O), from Na, acetonitrile (MeCN) from CaH_2 and dichloromethane (CH_2Cl_2) from P_2O_5.

The following chemicals were purchased from Aldrich and used as received: triphos; $NiCl_2 \cdot 6H_2O$; $NaBPh_4$, $SiMe_3Cl$, $PhCH_2MgCl$ (1 M solution), 4-$MeOC_6H_4CH_2Cl$ and 4-$MeC_6H_4CH_2Cl$. The compounds, $RC_6H_4CH_2MgCl$ (R = Me or MeO) [7] and [NiCl(triphos)]BPh_4 [5] were prepared by methods reported in the literature. $[NEt_4]Cl \cdot H_2O$ was purchased from Aldrich and dried by heating to 80 °C in vacuo overnight.

The compounds were characterised by ^1H NMR spectroscopy, ^{31}P NMR spectroscopy, elemental analysis and X-ray crystal structure determination. ^1H NMR and ^{31}P NMR spectroscopy was carried out on a 300 MHz Brüker NMR spectrometer fitted with a wide bore to hold larger NMR tubes, operating at 121.5 MHz. The samples were dissolved in deuterated, degassed solvents. Due to the low solubility and yield of the products, ^{31}P NMR spectroscopy needed to be performed overnight in order to increase the signal to noise ratio. The elemental analysis was carried out using a Carlo Erba elemental analyzer, model 1106. All X-ray crystal structures were obtained by the Newcastle University X-ray Crystallography Research Group.

2.1. Preparation of $[Ni(\eta^2\text{-}CH_2C_6H_4R\text{-}4)(triphos)]BPh_4$ (R = H, Me or MeO)

The series of complexes $[Ni(\eta^2\text{-}CH_2C_6H_4R\text{-}4)(triphos))]BPh_4$ were all prepared by the same method. The complexes were characterised by elemental and spectroscopic analysis as shown in Table 1, and by X-ray crystallography. A typical preparation is described below for $[Ni(\eta^2\text{-}CH_2C_6H_4OMe\text{-}4)(triphos)]BPh_4$.

A 1.5 M solution of 4-$MeOC_6H_4CH_2MgCl$ was prepared [7] in a two-neck, round-bottomed flask fitted with an efficient condenser and a dropping funnel by the slow addition of 4-$MeOC_6H_4CH_2Cl$ (25 g, 0.16 mol) in THF (50 mL) to a stirred mixture of magnesium turnings (4.2 g, 0.17 mol) in THF (50 mL).

Table 1
Elemental and spectroscopic characterisation of $[Ni(\eta^2\text{-}CH_2C_6H_4R\text{-}4)(triphos)]BPh_4$

R	Elemental analysis[a]/%		NMR spectroscopy [b]	
	C	H	^1H	^{31}P
H	77.8 (77.8)	5.3 (5.9)	7.2–8.3 (complex m, Ph groups) 6.2 (d, J_{HH} = 8.0 Hz, CH_2Ph) 2.1–2.7 (broad, CH_2CH_2)	87.7 (t, J_{PP} = 45 Hz, P_c) 47.5 (d, J_{PP} = 45 Hz, P_t)
Me	77.5 (77.9)	6.2 (6.1)	6.6-8.0 (complex m, Ph groups) 6.2 (d, J_{HH} = 9.6 Hz, CH_2Ar) 2.1–2.8 (broad, CH_2CH_2) 1.2 (s, CH_3)	88.8 (t, J_{PP} = 42 Hz, P_c) 47.7 (d, J_{PP} = 42 Hz, P_t)
MeO	76.4 (76.7)	6.00 (6.00)	6.8–7.8 (complex m, Ph groups) 6.5 (d, J_{HH} = 10.0 Hz, CH_2Ar) 6.15 (d, J_{HH} = 10.0 Hz, CH_2Ar) 3.65 (s, OCH_3) 2.1–2.8 (broad, CH_2CH_2)	86.3 (t, J_{PP} = 44.5 Hz, P_c) 45.3 (d, J_{PP} = 44.5 Hz, P_t)

[a] Calculated values shown in parentheses.
[b] Abbreviations: m = multiplet; t = triplet; d = doublet; s = singlet; P_c = central P in triphos; P_t = terminal P in triphos.

To a suspension of [NiCl(triphos)]BPh_4 (1 g, 1.95 mmol) in THF (ca. 30 mL) at −75 °C, an excess of 4-$MeOC_6H_4CH_2MgCl$ (10 mL, 15 mmol) was added slowly. The solution changed rapidly from orange to dark red and was stirred overnight. The next day, ethanol was added dropwise to the solution until there was no more effervescence. All volatiles were now removed in vacuo, to produce a red microcrystalline solid. The dry solid was extracted with the minimum amount of CH_2Cl_2 to form a red solution and a white solid. The magnesium salts were removed by filtration, washing with more CH_2Cl_2 to ensure complete extraction of the desired red product. Layering EtOH on the red solution produced (after several days of slow diffusion) red crystals of [Ni(η^2-$CH_2C_6H_4$OMe-4)(triphos)]BPh_4. The crystals were removed by filtration and dried in vacuo. The best yield obtained by this method was 35%. However, if the addition of the Grignard reagent to the [NiCl(triphos)]BPh_4 was performed at room temperature the maximum yield obtained was 11%.

On several occasions when we have prepared these complexes a mixture has been obtained consisting of orange and dark red crystals. Using NMR spectroscopy and X-ray crystallography it was shown evident that the red crystals are [Ni(η^2-$CH_2C_6H_4$OMe-4)(triphos)]-BPh_4 and the orange crystals are [NiCl(triphos)]BPh_4. The mixture can be separated as follows. Place the mixture in a sintered Schlenk flask and wash with 4 × 5 mL of MeCN whilst gently shaking. The [NiCl(triphos)]BPh_4 is much more soluble in MeCN than [Ni(η^2-$CH_2C_6H_4$OMe-4)(triphos)]BPh_4. When it was evident that no orange crystals were left, the red crystals were washed with a further 5 mL and dried in vacuo. Using this procedure the isolated yield of [Ni(η^2-$CH_2C_6H_4$OMe-4)(triphos)]BPh_4 is only ca. 3%.

2.2. X-ray crystallography

Data were measured on Bruker AXS SMART 1K and Nonius KappaCCD diffractometers at 150 K, using Mo Kα radiation (λ = 0.71073 Å), and semi-empirical absorption corrections were applied, based on repeated and symmetry-equivalent reflections. The structures were solved by direct and heavy-atom methods, and were refined on all unique F^2 values, with programs of the SHELX family (G.M. Sheldrick, University of Göttingen, Germany); anisotropic displacement parameters were refined for non-H atoms, and H atoms were refined as riding on their parent atoms in ideal geometry. For the benzyl complex with R = H, there are two independent cations and two anions in the asymmetric unit; the final difference map contains a significant peak close to one Ni atom, but no sensible disorder model was found to account for this. The structure of the benzyl complex with R = Me contains disordered solvent molecules, the exact nature of which could not be determined with confidence; although atomic sites could be assigned and refined as a mixture of carbon and oxygen, the geometry is not sensible for any recognisable solvent molecule, and so this has not been included in the formula of the compound. Solvent in the structure of the complex with R = OMe is even more disordered and could not be modeled with discrete atoms; instead, it was accounted for by the SQUEEZE procedure in PLATON (A.L. Spek, University of Utrecht, The Netherlands). The structure of [NiCl(triphos)]BPh_4 has two phenyl rings disordered over two orientations each in the cation.

Crystal data and other experimental information are given in Table 2. Selected bond lengths and angles for the three benzyl complexes are reported in Table 3. Crystallographic data for the structural analyses has been deposited with the Cambridge Crystallographic Data Centre: CCDC No. 249866 for [Ni(η^2-$CH_2C_6H_5$)-(triphos))]BPh_4; CCDC No. 249867 for [Ni(η^2-$CH_2C_6H_4$Me-4)(triphos))]BPh_4; CCDC No. 249868 for [Ni(η^2-$CH_2C_6H_4$OMe-4)(triphos))]BPh_4 and CCDC No. 249869 for [NiCl(triphos))]BPh_4.

2.3. Kinetic studies

All kinetic studies were performed using an Applied Photophysics SX.18MV stopped-flow spectrophotometer, modified to handle air-sensitive solutions. The temperature was maintained at 25.0 ± 0.1 °C using a Grant LT D6G thermostated recirculating pump.

All solutions were prepared under an atmosphere of dinitrogen and transferred by gas-tight, all-glass syringes into the stopped-flow spectrophotometer. Stock solutions of anhydrous HCl in MeCN were prepared by mixing equimolar amounts of $SiMe_3Cl$ and MeOH in the solvent. Dilute solutions containing mixtures of HCl and [NEt_4]Cl were prepared from the stock solutions of the two components. All solutions were prepared and used within 1 h.

Kinetics were studied under pseudo first-order conditions [8] with all reagents in a large excess (>10-fold) over the concentration of [Ni(η^2-$CH_2C_6H_4$R-4)(triphos)]BPh_4. Under all conditions the absorbance-time curve for the reactions is an excellent fit to a single exponential for at least 4 half-lives, indicating a first-order dependence on the concentration of complex. The entire curve was fitted using the Applied Photophysics computer program to obtain the observed rate constants (k_{obs}). The rate laws were determined by graphical analysis as described in Section 3.

2.4. Characterisation of the product of protonation

The reaction of an excess of anhydrous HCl with all [Ni(η^2-$CH_2C_6H_4$R-4)(triphos)]$^+$ produced [NiCl(triphos)]$^+$. The product was characterised in situ by ^{31}P NMR spectroscopy {δ110.2 (t, J_{PP} = 49.6 Hz, P_c);

Table 2
Crystal data and structure refinement parameters for [Ni($CH_2C_6H_4$R-4)(triphos)]BPh_4 (R = H, Me or MeO) and [NiCl(triphos)]BPh_4

	[Ni($CH_2C_6H_5$)(triphos)]-BPh_4	[Ni($CH_2C_6H_4$Me-4)(triphos)]-BPh_4	[Ni($CH_2C_6H_4$OMe-4)(triphos)]-BPh_4	[NiCl(triphos)]-BPh_4
Chemical formula	$C_{65}H_{60}BNiP_3$	$C_{66}H_{62}BNiP_3$	$C_{66}H_{62}BNiOP_3$	$C_{58}H_{53}BClNiP_3$
Fw	1003.6	1017.6	1033.6	947.9
Crystal system	Triclinic	Monoclinic	Monoclinic	Triclinic
Space group	$P\bar{1}$	$P2_1/n$	$P2_1/n$	$P\bar{1}$
T (K)	150	150	150	150
a (Å)	18.4171(8)	13.6232(16)	13.6171(6)	11.4983(5)
b (Å)	18.6374(8)	19.860(2)	19.9305(9)	14.3108(6)
c (Å)	19.6767(9)	20.622(3)	20.5807(9)	17.0594(7)
α (°)	65.798(2)	90	90	98.102(2)
β (°)	69.175(2)	104.888(9)	103.266(2)	105.120(2)
γ (°)	61.155(2)	90	90	112.220(2)
V (Å^3)	5289.8(4)	5392.2(11)	5436.5(4)	2416.9(2)
Z	4	4	4	2
Reflections measured	38,266	32,359	31,534	17,734
Unique data, R_{int}	18,369, 0.048	6970, 0.085	7108, 0.062	8461, 0.027
Parameters	1261	661	651	670
R [$F^2 > 2\sigma$]	0.047	0.046	0.041	0.035
R_w (F^2, all data)	0.118	0.094	0.103	0.089
Goodness-of-fit [F^2]	0.997	1.083	1.021	1.050
Maximum, minimum electron density (e/Å^3)	1.80, −0.79	0.33, −0.31	0.39, −0.29	0.42, −0.40

Table 3
Selected bond lengths (Å) and angles (°) for [Ni(η^2-$CH_2C_6H_4$R-4)(triphos)]BPh_4

R	Bond lengths					Bond angles		
	Ni–P_t	Ni–P_c	Ni–CH_2	Ni–C_{ipso}	CH_2–C_{ipso}	Ni–CH_2–C_{ipso}	CH_2–Ni–C_{ipso}	P_t–Ni–P_t
H	2.1813(9)	2.2040(9) 2.1694(9)	1.970(3)	2.484(3)	1.448(5)	91.9(2)	35.6(2)	138.19(4)
	2.2112(9)	2.2104(10) 2.1844(10)	1.991(3)	2.335(3)	1.458(5)	83.7(2)	38.3(2)	137.38(4)
Me	2.1899(11)	2.2425(10) 2.1897(10)	1.974(3)	2.263(4)	1.466(5)	80.8(2)	39.74(14)	129.75(4)
MeO	2.1896(9)	2.2280(10) 2.1967(10)	1.966(3)	2.250(3)	1.459(4)	80.65(18)	39.78(12)	129.93(4)

δ48.7 (d, J_{PP} = 49.6 Hz, P_t)} and visible absorption spectroscopy (λ_{max} = 330 nm, $\varepsilon_{330} = 1.34 \times 10^3$ dm^3 mol^{-1} cm^{-1}; λ_{max} = 450 nm, ε_{450} = 500 dm^3 mol^{-1} cm^{-1}). The spectra were identical to those of an authentic sample of [NiCl(triphos)]BPh_4 prepared by the method described in the literature [5].

The X-ray crystal structure of [NiCl(triphos)]BPh_4 has also been determined. The structure of the cation is shown in Fig. 1 and is as anticipated. The geometry about the nickel is best described as distorted square-planar. The bond distance of the phosphorus trans to the chloride ligand, Ni–P(2) (2.1191 (6) Å), is shorter than the Ni–P(1) (2.2096(7) Å) and Ni–P(3) (2.1956(7) Å) bond distances, possibly due to the electronegative chloride ligand donating electron density to the nickel, which in turn increases the π-back bonding to the *trans* phosphorus, shortening the Ni–P(2) bond.

3. Results and discussion

3.1. Synthesis of [Ni(η^2-$CH_2C_6H_4$R-4)(triphos)]BPh_4

The complexes [Ni(η^2-$CH_2C_6H_4$R-4)(triphos)]BPh_4 were prepared by the reaction shown in Eq. (2). Attempts to improve the poor yields by: (i) using various proportions of the Grignard to [NiCl(triphos)]BPh_4, from equimolar amounts to a large excess of the Grignard; (ii) performing the reaction in thf or diethyl ether; (iii) performing the reaction at −78 °C or (iv) using a variety of alcohols (Pr^iOH, EtOH or MeOH) to destroy the excess of the Grignard reagent, resulted in the best isolated yield of ca. 35%. In addition, leaving the solution in the freezer, or adding a greater excess of MeOH, to facilitate crystallization had no significant effect on the yield.

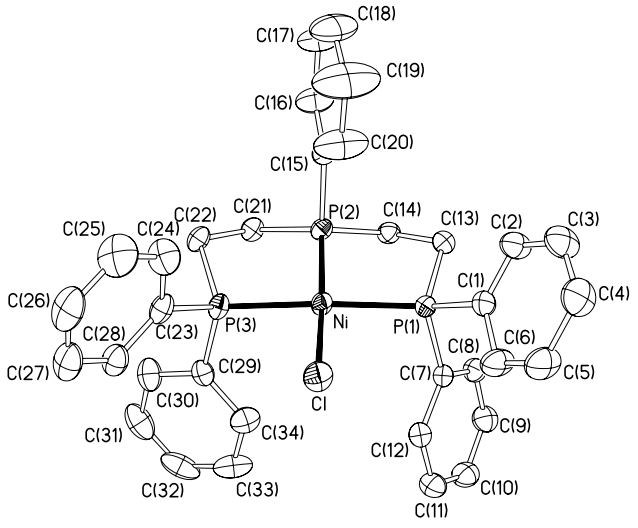

Fig. 1. Structure of the cation in [NiCl(triphos)]BPh_4 with 50% probability displacement ellipsoids. Hydrogen atoms and minor disorder components are omitted. Selected bond lengths are: Ni–P(1) = 2.2096(7); Ni–P(3) = 2.1956(7); Ni–P(2) = 2.1191(6) Å. Selected bond angles are: P(1)–Ni–P(2) = 85.75(2); P(1)–Ni–P(3) = 162.74(3); P(2)–Ni–P(3) = 85.60(2); Cl–Ni–P(1) = 97.28(3); Cl–Ni–P(2) = 171.66(3); Cl–Ni–P(3) = 93.37(3)°.

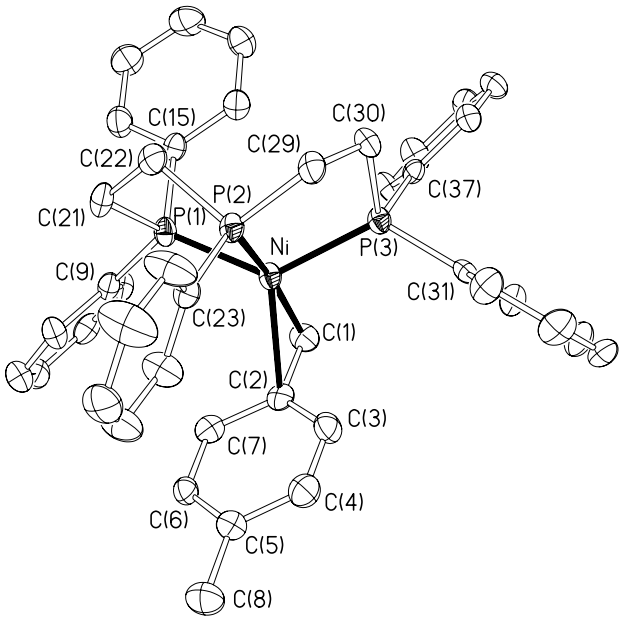

Fig. 2. Structure of [Ni(η^2-$CH_2C_6H_4Me$)(triphos)]$^+$ with 50% probability displacement ellipsoids. Hydrogen atoms are omitted.

$$[NiC(triphos)]BPh_4 \xrightarrow{4\text{-}RC_6H_4CH_2MgCl} [Ni(\eta^2\text{-}CH_2C_6H_4R\text{-}4)(triphos)]BPh_4 \quad (2)$$

We have been unable to extend the range of [Ni(η^2-$CH_2C_6H_4R$-4)(triphos)]BPh_4 to include benzyl derivatives where R is an electron-withdrawing substituent (e.g. 4-$O_2NC_6H_4CH_2$- or 4-$ClC_6H_4CH_2$–) because of the inability to prepare the necessary Grignard reagents.

All [Ni(η^2-$CH_2C_6H_4R$-4)(triphos)]BPh_4 (R = H, Me or MeO) were characterised by ^1H and ^{31}P NMR spectroscopy, elemental analysis and X-ray crystallography. Most notably, the X-ray crystal structures unambiguously demonstrate that the substituted benzyl ligands bind to the nickel in what is best described as an η^2-coordination mode. We will discuss the crystallography of these complexes first and then present the NMR spectroscopic information.

3.2. Structures of [Ni(η^2-$CH_2C_6H_4R$-4)(triphos)]BPh_4

X-ray crystallographic investigation of [Ni(η^2-$CH_2C_6H_4R$-4)(triphos)]BPh_4 (R = H, Me or MeO) shows that all the cations have similar structures typified by that of [Ni(η^2-$CH_2C_6H_4Me$-4)(triphos)]$^+$ shown in Fig. 2. The geometry at the nickel is best described as distorted square-planar. Three of the four coordination sites are occupied by the phosphorus atoms of the triphos ligand and the fourth site corresponds to the centre of the CH_2–C_{ipso} bond. The CH_2–C_{ipso} bond is orientated perpendicular to the coordination plane of the complex. In all the structures the phenyl group on the central phosphorus is orientated in the same direction as the phenyl group of the benzyl ligand. This orientation minimises unfavourable steric interactions of the benzyl group with the phenyl groups on the terminal phosphorus atoms.

Whilst the majority of benzyl ligands coordinate in an end-on configuration, other binding modes are known, such as η^2- and η^3-coordination [9]. The dimensions of the Ni-benzyl group in [Ni(η^2-$CH_2C_6H_4R$-4)(triphos)]$^+$ demonstrate that the benzyl ligand is bound in the η^2-configuration. The unusually short distance between nickel and the ipso-carbon on the benzyl ligand {R = H: Ni–C_{ipso} = 2.484(3) and 2.335(3); R = Me: Ni–C_{ipso} = 2.263(4); R = MeO: Ni–C_{ipso} = 2.250(3)} strongly indicates an interaction in all cases, as do the Ni–CH_2–C_{ipso} angles, which are small {R = H: angle = 91.9(2) and 83.7(2)°; R = Me: angle = 80.8(2); R = MeO: angle = 80.65(18)°}. In transition metal benzyl complexes showing no evidence of a M–C_{ipso} interaction the M–CH_2–C_{ipso} angle is closer to the tetrahedral angle of 109.5°. The nickel-C_{ortho} distance in all the complexes is too large for any interaction, thus precluding an η^3-benzyl coordination. Further evidence that the η^2-benzyl description is correct comes from considerations of the bond lengths within the benzyl ligand.

A typical CH_3–C_6H_4R single bond length [10] is 1.53 ± 0.01 Å. The CH_2–C_{ipso} bond lengths in the [Ni(η^2-$CH_2C_6H_4R$-4)(triphos)]$^+$ complexes are 0.05–0.08 Å shorter, suggesting partial double bond character (R = H: CH_2–C_{ipso} = 1.448(5) and 1.458(5); R = Me: CH_2–C_{ipso} = 1.466(5); R = MeO: CH_2–C_{ipso} = 1.459(4) Å). The phenyl ring is coplanar with the CH_2 carbon atom, and the benzyl ligand lies approximately perpendicular to the Ni–CH_2–C_{ipso} triangle.

3.3. Spectroscopic characterisation

The ^{1}H NMR spectra of all the complexes [Ni(η^2-$CH_2C_6H_4$R-4)(triphos)]BPh_4 are similar. The aromatic region is very complicated because of the large number of various phenyl groups on the triphos ligand, the $[BPh_4]^-$ and the benzyl ligand. However, the ^{1}H NMR spectra of [Ni(η^2-$CH_2C_6H_4$Me-4)(triphos)]BPh_4 and [Ni(η^2-$CH_2C_6H_5$)(triphos)]BPh_4 both show a doublet at δ 6.2. We tentatively suggest that this peak is assigned to the methylene protons of C_{ipso} coupled to the central P of the triphos ligand. The central P is essentially *trans* to the benzyl ligand. If this assignment is correct, we must conclude that coupling to the two terminal P (which are effectively *cis* to the benzyl ligand) is too small to be detected. [Ni(η^2-$CH_2C_6H_4$OMe-4)(triphos)]BPh_4 shows two doublets (δ 6.15 and δ 6.50). The singlet at δ 3.65 in the spectrum of [Ni(η^2-$CH_2C_6H_4$OMe-4)(triphos)]BPh_4 is assigned to the three protons on the methoxy group, and the singlet at δ 1.2 in the spectrum of [Ni(η^2-$CH_2C_6H_4$Me-4)(triphos)]BPh_4 is assigned to the methyl group.

Further evidence for the Ni–C_{ipso} interaction comes from the noticeable downfield shift of the CH_2–C_{ipso} peaks in the ^{1}H NMR spectrum. Formation of a metallocycle results in additional ring current which opposes the external field, deshielding the proton. An agostic interaction with the aromatic residue of the type C–H···M can be excluded. This type of interaction would result in a high-field shift [11].

All the spectroscopic data is consistent with the structures of [Ni(η^2-$CH_2C_6H_4$MR-4)(triphos)]$^+$ having the same structure in solution as established in the X-ray crystal structures: the benzyl ligand lies approximately perpendicular to the Ni–CH_2–C_{ipso} triangle.

3.4. Kinetics and mechanism of the reaction between [Ni(η^2-$CH_2C_6H_4$R-4)(triphos)]$^+$ and HCl

The reaction of an excess of anhydrous HCl with [Ni(η^2-$CH_2C_6H_4$R-4)(triphos)]$^+$ (R = H, Me or MeO) in MeCN produces [NiCl(triphos)]$^+$ and 4-RC_6H_4Me, as described by Eq. (3). The kinetics have been monitored by stopped-flow spectrophotometry, with both HCl and Cl^- present in a large excess over the concentration of the complex. MeCN was chosen as the solvent because of the extensive data concerning acid strengths and homoconjugation equilibria which are known in this solvent [12]. Under all conditions, the absorbance–time curve can be fitted to a single exponential, with the initial absorbance corresponding to that of [Ni(η^2-$CH_2C_6H_4$R-4)(triphos)]$^+$ and the final absorbance to that of [NiCl(triphos)]$^+$. The observed rate constant (k_{obs}) depends on the ratio [HCl]/[Cl^-] as shown in Fig. 3. The kinetics of the reactions of all [Ni(η^2-$CH_2C_6H_4$R-4)(triphos)]$^+$ (R = H, Me or MeO) can be accommodated by the rate law shown in Eq. (4), ($R = H : k_2^H = 0.71 \pm 0.04\ s^{-1}$; $R = Me : k_2^{Me} = 0.20 \pm 0.03\ s^{-1}$; $R = MeO : k_2^{MeO} = (2.1 \pm 0.5) \times 10^{-3}\ s^{-1}$).

$$[Ni(\eta^2\text{-}CH_2C_6H_4R\text{-}4)(triphos)]^+ + HCl \rightarrow [NiCl(triphos)]^+ + 4\text{-}CH_3C_6H_4R \quad (3)$$

$$\frac{-d[Ni(CH_2C_6H_4R\text{-}4)(triphos)^+]}{dt} = k_2^R \frac{[HCl]}{[Cl]^-}[Ni(CH_2C_6H_4R\text{-}4)(triphos)]^+ \quad (4)$$

The analysis of the kinetic data needs some further explanation. When studying the reaction of compounds with HCl in acetonitrile there is the problem of whether the reacting acid is HCl or solvated H^+ {Eq. (5)}.

$$HCl \overset{K_a^{HCl}}{\rightleftharpoons} H^+ + Cl^- \quad (5)$$

Clearly, the addition of Cl^- to solutions of HCl in MeCN will perturb the concentration of solvated H^+ (K_a^{HCl}) according to Eq. (5). However, the addition of Cl^- to solutions of HCl in MeCN also perturbs the concentration of HCl because of the formation of $[HCl_2]^-$ according to the homoconjugation equilibrium (K_H) shown in Eq. (6). Using the literature values [12,13] of $K_H = 158.5\ dm^3\ mol^{-1}$ with $K_a^{HCl} = 1.3 \times 10^{-9}\ dm^3\ mol^{-1}$ we have calculated the concentrations of HCl, Cl^- and H^+ as shown in Table 4. The values of [HCl]/[Cl^-] shown in Fig. 3 are those corrected for the homoconjugation equilibrium.

$$HCl + Cl^- \overset{K_H}{\rightleftharpoons} HCl_2^- \quad (6)$$

The kinetics shown in Eq. (4) could represent, not a dependence on [HCl]/[Cl^-], but actually a dependence on [H^+] as shown in Eq. (7), where $k_H^R = k_2^R/K_a^{HCl}$. If Eq. (7) were the true form of the rate law, and the kinetics exhibit a dependence on the concentration of H^+, $k_H^H = 5.5 \pm 0.3 \times 10^8\ dm^3\ mol^{-1}\ s^{-1}$, $k_H^{Me} = 1.5 \pm 0.2 \times 10^8\ dm^3\ mol^{-1}\ s^{-1}$ and $k_H^{MeO} = 1.6 \pm 0.3 \times 10^6\ dm^3\ mol^{-1}\ s^{-1}$. Whilst these second order rate constants are fast they are slower than the diffusion-controlled limit ($k = 1 \times 10^{10}\ dm^3\ mol^{-1}\ s^{-1}$), and hence not unreasonable even for a mechanism involving a rate-limiting protonation step. Based on the kinetics, we cannot establish whether the true (mechanistically significant) form of the rate law is Eq. (4) or (7).

$$\frac{-d[Ni(CH_2C_6H_4R\text{-}4)(triphos)^+]}{dt} = k_H^R[H^+][Ni(CH_2C_6H_4R\text{-}4)(triphos)^+] \quad (7)$$

In the case of [Ni(η^2-$CH_2C_6H_4$OMe-4)(triphos)]$^+$ the quality of the kinetic data is poor. Because of the scatter of the data, the non-zero intercept shown in Fig. 3

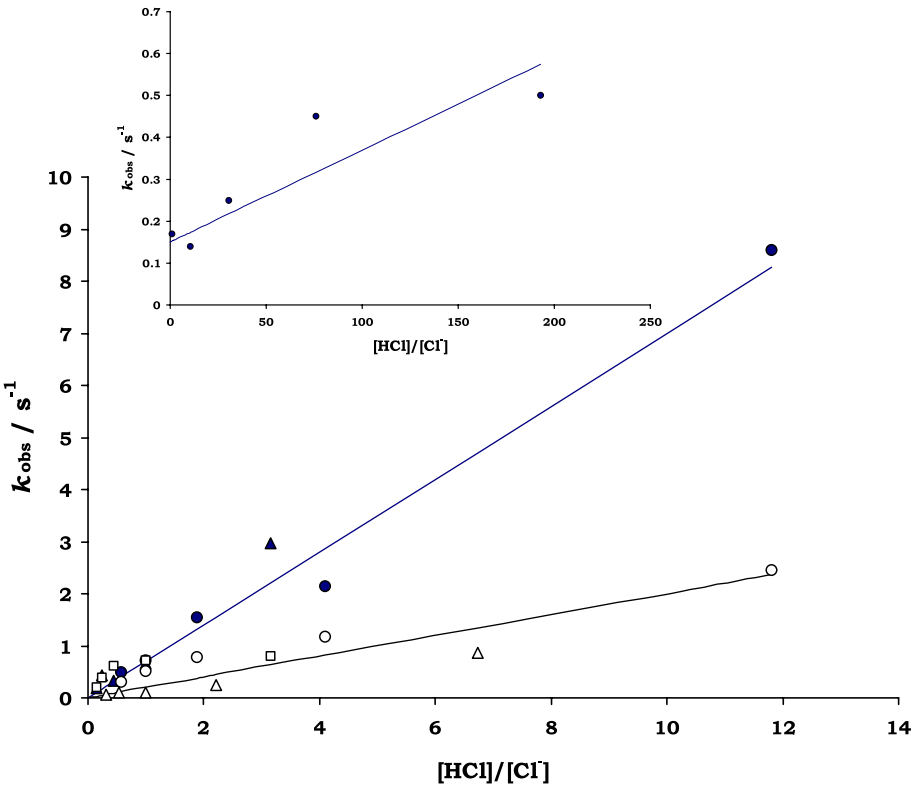

Fig. 3. Kinetic data for the reactions between $[Ni(\eta^2\text{-}CH_2C_6H_4R)(triphos)]^+$ (R = H, Me or MeO) and HCl in MeCN at 25.0 °C. *Main*. Dependence of k_{obs} on the ratio, [HCl]/[Cl⁻] for the reactions of R = H (full symbols) and R = Me (open symbols). The data points correspond to: [HCl] = 20 mmol dm^{-3}, [Cl⁻] = 5–25 mmol dm^{-3} (●); [HCl] = 10 mmol dm^{-3}, [Cl⁻] = 5–25 mmol dm^{-3} (▲); [HCl] = 20 mmol dm^{-3}, [Cl⁻] = 5–25 mmol dm^{-3} (○); [HCl] = 15 mmol dm^{-3}, [Cl⁻] = 5–25 mmol dm^{-3} (△); [HCl] = 10 mmol dm^{-3}, [Cl⁻] = 5–25 mmol dm^{-3} (□). *Insert* Dependence of k_{obs} on the ratio, [HCl]/[Cl⁻] for the R = MeO derivative. The data points correspond to: [HCl] = 50 mmol dm^{-3}, [Cl⁻] = 2–50 mmol dm^{-3} (●). In all cases the concentrations of HCl and Cl⁻ have been corrected for the homoconjugation equilibrium shown in Eq. (6). The lines drawn are those defined by Eq. (4) and the values presented in the text.

(insert) may be meaningless and we conclude that the rate law, even for this derivative, is that shown in Eq. (4). The reason for the poor quality of the kinetic data with the R = MeO derivative is not clear.

3.5. The mechanism of the reactions of $[Ni(\eta^2\text{-}CH_2C_6H_4R\text{-}4)(triphos)]^+$ with HCl

The simplest interpretation of the rate law shown in Eq. (4) is that the mechanism involves protonation of the benzyl carbon followed by dissociation of the substituted toluene. However, it is difficult to reconcile such a simple protonation mechanism with the effect that the 4-R-substituent has on the rates of the reactions: as the 4-R-substituent becomes more electron-releasing, the reaction becomes slower (R = H > Me > MeO). It is not easy to see how the rate of a simple protonation of a carbon site would be facilitated by 4-R-substituents which make the carbon site less basic.

It is proposed that the mechanism could involve initial rapid protonation of the nickel. Subsequent product formation could then occur by migration of the hydrogen from the nickel to the coordinated benzyl as shown in Fig. 4. The rate law associated with this mechanism is shown in Eq. (8), and is derived assuming that $[NiH(\eta^2\text{-}CH_2C_6H_4R\text{-}4)(triphos)]^{2+}$ is a steady state intermediate. If $k^R_{-3} > k^R_4$ then Eq. (8) simplifies to Eq. (9), which is identical in form to that observed experimentally {Eq. (4)}. Comparison of Eqs. (4) and (9) yields the values of $k^R_3 k^R_4 / k^R_{-3} = k^R_2$ shown in Table 5.

$$\frac{-d[Ni(\eta^2\text{-}CH_2C_6H_4R\text{-}4)(triphos)^+]}{dt} = \frac{k^R_4 k^R_3 [HCl]}{k^R_4 + k^R_{-3}[Cl^-]}[Ni(\eta^2\text{-}CH_2C_6H_4R\text{-}4)(triphos)^+] \quad (8)$$

$$\frac{-d[Ni(\eta^2\text{-}CH_2C_6H_4R\text{-}4)(triphos)^+]}{dt} = \frac{k^R_4 k^R_3 [HCl]}{k^R_{-3}[Cl^-]}[Ni(\eta^2\text{-}CH_2C_6H_4R\text{-}4)(triphos)^+] \quad (9)$$

The overall effect that the 4-R-substituents have on the rate of the reaction depends on the effect that the 4-R-substituent has on the individual elementary rate constants k^R_3, k^R_4 and k^R_{-3}. It seems intuitively reasonable

Table 4
Kinetic data for the reactions of HCl with [Ni(η^2-$CH_2C_6H_4$R-4)(triphos)]BPh_4 (R = H, Me or MeO) in the presence of Cl^- in MeCN at 25.0 °C

R	[HCl] (mmol dm^{-3})	[Cl^-] (mmol dm^{-3})	[HCl]$_e$[a] (mmol dm^{-3})	[Cl^-]$_e$[a](mmol dm^{-3})	[H^+] (10^9 mol dm^{-3})	k_{obs} (s^{-1})
H	10.0	5.0	7.31	2.31	42.5	3.0
		10.0	5.39	5.39	1.26	0.62
		15.0	4.09	9.09	0.567	0.32
		20.0	3.23	13.23	0.307	0.44
		25.0	2.67	17.67	0.190	0.19
	20.0	5.0	16.39	1.39	14.9	8.6
		10.0	13.2	3.2	5.16	2.20
		15.0	10.6	5.64	2.38	1.55
		20.0	8.46	8.46	1.26	0.73
		25.0	6.9	11.9	0.73	0.49
Me	10.0	5.0	7.31	2.31	42.5	0.81
		10.0	5.39	5.39	1.26	0.72
		15.0	4.09	9.09	0.567	0.62
		20.0	3.23	13.23	0.307	0.39
		25.0	2.67	17.67	0.190	0.21
	15.0	5.0	11.74	1.74	8.51	0.86
		10.0	9.39	4.39	2.69	0.25
		15.0	7.09	7.09	1.26	0.10
		20.0	5.64	10.64	0.668	0.09
		25.0	4.5	14.5	0.391	0.06
Me	20.0	5.0	16.39	1.39	14.9	2.46
		10.0	13.2	3.22	5.16	1.18
		15.0	10.6	5.64	2.38	0.79
		20.0	8.46	8.46	1.26	0.51
		25.0	6.9	11.9	0.73	0.31
MeO	50.0	2.0	48.25	0.25	243	0.50
		5.0	45.6	0.60	95.8	0.45
		10.0	41.35	1.35	38.6	0.25
		20.0	33.2	3.2	13.1	0.14
		50.0	14.8	14.8	1.26	0.17

[a] Concentrations calculated allowing for homoconjugation equilibrium.

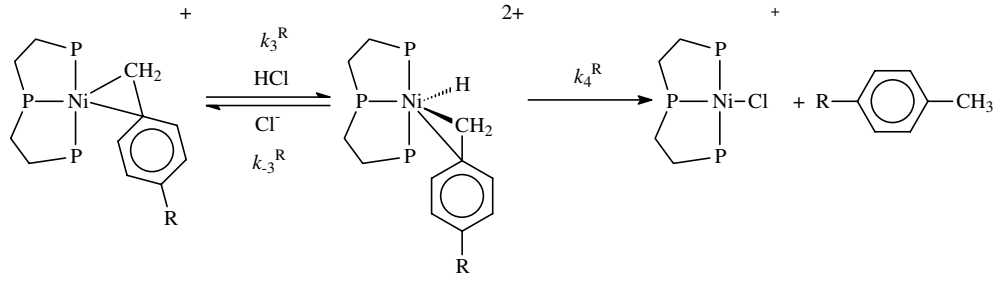

Fig. 4. The mechanism of the reactions between [Ni(η^2-$CH_2C_6H_4$R)(triphos)]$^+$ (R = H, Me or MeO) and HCl in MeCN. The mechanism is only shown for HCl being the acid. An analogous mechanism could be drawn for H^+ being the acid.

that the protonation step k_3^R is facilitated by electron-releasing 4-R-substituents, and deprotonation k_{-3}^R would be slower with electron-releasing R, since such 4-R-substituents would increase the electron-richness of the nickel site. The observation that electron-withdrawing substituents facilitate the reaction must be attributable to the effect of the 4-R-substituent on the unimolecular k_4^R step. If the k_4^R step involved *intramolecular hydride transfer*, electron-withdrawing 4-R-substituents would stabilize the transition state by neutralizing the build-up of negative charge on the methylene group. A similar argument has been presented for the reactions involving intramolecular hydrogen migration reactions of *exo*- and *endo*-[Nb(η^5-C_5H_5)$_2$H(CH_2 = CHC_6H_4R-4)]. It has

Table 5
Summary of the elementary rate for the reactions of [Ni(η^2-$CH_2C_6H_4$-R-4)(triphos)]$^+$ with HCl in MeCN at 25.0 °C

R	$k_3^R k_4^R / k_{-3}^R$ ($dm^3\ mol^{-1}\ s^{-1}$)
H	0.70 ± 0.10
Me	0.21 ± 0.05
MeO	$(2.2 \pm 0.8) \times 10^{-3}$

been observed that electron-releasing 4-R-substituents accelerate migration [14], presumably by stabilizing the modest accumulation of positive charge at C_β in the transition state for the migration.

3.6. Mechanisms of the reactions of [NiR(triphos)]$^+$ with HCl

The kinetics and mechanism of the reactions of [Ni(η^2-$CH_2C_6H_4$R-4)(triphos)]$^+$ with HCl described in this paper are markedly different to those observed in the earlier study on [NiMe(triphos)]$^+$. Both systems appear to protonate preferentially at the nickel. However, in the benzyl complexes the subsequent formation of products involves migration of the hydride from nickel to benzyl ligand, but in [Ni(H)Me(triphos)]$^{2+}$ product formation has to await the addition of a second proton (presumably at the methyl ligand) [4]. What controls how [Ni(H)R(triphos)]$^{2+}$ converts into products (migration or additional protonation) is currently not clear. However, it seems likely that the additional protonation pathway is observed with more basic alkyl ligands (e.g. Me ligand), whereas with less basic ligands (e.g. benzyl) the migration pathway operates.

Acknowledgement

One of us (V.A.) thanks the University of Newcastle for a studentship.

References

[1] (a) C. Masters, Homogeneous Transiton Metal Catalysis, Chapman and Hall, London, 1981, pp. 135–158;
(b) P.W. Jolly, G. WilkeOrganic Chemistry of Nickel, vol. 2, Academic Press, New York, 1975;
(c) R.A. Henderson, J. Chem. Res. (S) (2002) 407.
[2] (a) K.W. Kramarz, J.R. Norton, Prog. Inorg. Chem. 42 (1994) 1;
(b) R.A. Henderson, Angew. Chemie, Int. Ed. 35 (1996) 946;
(c) S.S. Kristjansdottir, J.R. Norton, in: A. Dedieu (Ed.), Transition Metal Hydrides: Recent Advances in Theory and Experiment, 1992 (chapter 9);
(d) E.T. Papish, M.P. Magee, J.R. Norton, in: M. Peruzzini, R. Poli (Eds.), Recent Advances in Hydride Chemistry, Elsevier, Amsterdam, 2001 (chapter 2).
[3] R.A. Henderson, J. Chem. Soc. Dalton Trans. (1995) 503.
[4] R.A. Henderson, K.E. Oglieve, Chem. Commun. (1999) 2271.
[5] W. Clegg, G. Cropper, R.A. Henderson, C. Strong, B. Parkinson, Organometallics 20 (2001) 2579.
[6] (a) W. Clegg, R.A. Henderson, Inorg. Chem. 41 (2002) 1128;
(b) V. Autissier, P.M. Zarza, A. Petrou, R.A. Henderson, R.W. Harrington, W. Clegg, Inorg. Chem. 43 (2004) 3106.
[7] A.I. Vogel, Textbook of Practical Organic Chemistry, third ed., Longmans, London, 1967, 812 pp.
[8] J.H. Espenson, Chemical Kinetics and Reaction Mechanisms, McGraw-Hill, New York, 1981, pp. 30–32.
[9] (a) Selected examples of structures of benzyl-complexes are: N.H. Dryden, P. Legzdins, J. Trotter, V.C. Yee, Organometallics 10 (1991) 2857;
(b) C. Pellecchia, A. Grassi, A. Immirzi, J. Am. Chem. Soc. 115 (1993) 1160;
(c) W. Clegg, M.R.J. Elsegood, P.W. Dyer, V.C. Gibson, E.L. Marshall, Acta Cryst. 55 (1999) 916;
(d) W. Lesueur, E. Solari, C. Floriani, Inorg. Chem. 36 (1997) 3354.
[10] See Ref. [9a].
[11] M. Brookhart, M.L.H. Green, L. Wong, Prog. Inorg. Chem. 36 (1988) 1.
[12] K. Izutsu, Acid–Base Dissociation Constants in Dipolar Aprotic Solvents, Blackwell Scientific, Oxford, 1990.
[13] J.F. Coetzee, Prog. Phys. Org. Chem. 4 (1967) 45.
[14] B.J. Burger, B.D. Santarsiero, M.S. Trimmer, J.E. Bercaw, J. Am. Chem. Soc. 110 (1988) 3134.